PAPER Nr.: 108

ANALYSIS OF ORTHOTROPIC BEAMS OF SOLID CROSS-SECTIONS

BY

O. RAND

DEPARTMENT OF AEROSPACE ENGINEERING
TECHNION - ISRAEL INSTITUTE OF TECHNOLOGY
HAIFA 32000, ISRAEL

TWENTIETH EUROPEAN ROTORCRAFT FORUM
OCTOBER 4 - 7, 1994 AMSTERDAM

Printed by the Technical Highschool Haarlem

ANALYSIS OF ORTHOTROPIC BEAMS OF SOLID CROSS-SECTIONS

O. Rand
Department of Aerospace Engineering
Technion - Israel Institute of Technology
Haifa 32000, Israel

Abstract

The paper presents a nonlinear formulation and a finite-differences based numerical solution for the structural behavior of generic orthotropic beams of solid cross-sections. The analysis includes a detailed description of the three-dimensional out-of-plane warping and the solution is achieved by successive iterations while preserving all geometrical nonlinearities. The axial body force is introduced consistently through the axial differential equilibrium equation. The formulation yields some basic closed-form analytic solutions for homogeneous beams, and the numerical results provide an insight into the coupling effects mechanisms in generic laminated composite beams, including the resulting interlaminar stresses.

Introduction

The structural behavior of composite beams has attracted considerable research attention during the last years. There are many engineering applications where primary structures are designed as beams. Helicopter blades, propellers, wind turbine blades, wings and space structures are in this category.

The modern composite materials technology offers many advantages. Using advanced manufacturing techniques, fiber-reinforced designs offer weight reduction for given strength requirements and increasing of fatigue life. However, there are many applications where the structural coupling effects which are offered by composite materials are much more attractive. An excellent example of beam structures which may benefit from such structural couplings are helicopter blades. A specific example of a favorable coupling effect in helicopter blades is the so called "flap-pitch" coupling. It turns out that such coupling may improve the stability characteristics of helicopter blades and proportors blades. In isotropic blades, this coupling may be introduced by external mechanisms which could be eliminated by using composite materials. Such aeroelastic tailoring has already proved to be feasible - see for example Refs. 1,2. Currently, most of the helicopter blades are built as thin-walled structures. However, the use of composite materials seems to lessen weight considerations and utilizing blades of solid spar may be possible. Also, the manufacturing process of such blades seems to be simpler.

Presented at the 20th European Rotorcraft Forum, 4-7 October 1994, Amsterdam, The Netherlands.

From the analysis point of view, composite materials offer many design variations. These additional degrees of freedom make the analyses of composite beams much more complicated then those of isotropic beams. Generally, it may be stated that the main difference lays in the inability to bypass the need to determine the cross-sectional warping effects in composite beams. This is due to the fact that composite materials in general, and in particular orthotropic composite materials, couple shear strains with normal stresses and normal strains with shear stresses. Thus, a detailed description of shear stresses and therefore shear deformation is inevitable. In isotropic beams, shear deformation is ignored by adopting the well known Bernoulli-Euler assumptions. This enables the expression of the cross-sectional resultant shear forces as derivatives of the cross-sectional resultant moments which are expressed solely by the normal stresses.

Currently, many of the existing published analyses are based on the finite-element method. Reference 3 presents a review and discussion of existing methods for analyzing rotor blades and the variety of their assumptions. Aspects of geometrical nonlinearities in beams are also extensively dealt with in the literature. These aspects are discussed in Ref. 4, which also presents the three-dimensional nonlinear equations of motion of an isotropic Bernoulli-Euler beam. Since the literature contains many beam-plate models (i.e. beams which are essentially thin plates of high aspect ratio), the reader is also referred to a review of recent developments in the analysis of laminated beams presented in Ref. 5, which also discusses the various shear-deformation theories and the relevant finite-element models.

Generally, the advanced analyses may be divided into three categories. The first category includes models which consistently include all the necessary ingredients of the problem (Refs. 6-9). The second category consists of analyses where warping is expanded into a series of auxiliary warping functions (Refs. 10,11). The third category includes analyses which are based on a priori determination of the cross-sectional properties (stiffness, shear centers etc.) which are introduced to a standard one-

dimensional beam model (Ref. 12-14). Detailed discussion of the above models may be found in Ref. 15.

The purpose of the present paper is to present a new formulation and solution method for predicting the nonlinear behavior of composite beams having solid cross-sections. The beam-like behavior assumption (which is usually expected in slender structures) is used only for the formulation of the transverse displacements and the twist, while generic three-dimensional out-of-plane warping is included. The finite-differences based numerical procedure provides the ability to include all three-dimensional effects and all nonlinear terms with no neglect or use of an ordering scheme, and makes no use of two-dimensional cross-sectional properties. The iterative nature of the solution procedure enables the inclusion of a large number of degrees of freedom and to gradually adapt the numerical mesh during iterations. It should be emphasized that the present model is not limited to thin cross-sections and that all contributions to shear deformation are included in the warping function regardless their source (i.e. transverse shear or torsion). This enables consistent fulfillment of the cross-sectional boundary conditions by assuring no shear stresses normal to the contour. Since the present formulation provides detailed distribution of shear deformation and stresses, it also provides data concerning the resulting interlaminar stresses.

Analysis

An orthotropic, slender and uniform beam having solid cross-section is presented in Fig. 1. A basic reference system is defined by the coordinate lines x, y, z. The x coordinate line will be referred to as the"beam axis"and is assumed to pass through the same arbitrary point at each cross-section. The beam is assumed to be made out of orthotropic lamina where one plane of material symmetry is parallel to the x-y plane and the other plane is parallel to the z coordinate line. The displacements are expressed by four unknown longitudinal functions, in addition to a three-dimensional function. Referring to the notation of Fig. 1, u(x) is the blade axial displacement (in the x direction), and v(x) and w(x) are two transverse displacements in the y and z directions, respectively. These displacements take a point P on the beam axis to its position after deformation, P'. In addition, a twist angle $\phi(x)$ is assumed to take place around the deformed axis (i.e about the beam axis in its deformed direction due to the u,v and w displacements - see Fig. 1). $\psi(x,y,z)$ is a generic out-of-plane warping function which is superimposed on the axial displacement in the deformed axis direction and has zero averaged value over each cross-section. To facilitate the following derivation, two additional cross-sectional systems of coordinates should be defined. $\hat{x}_B$, $\hat{y}_B$, $\hat{z}_B$ are unit vectors of a local system of coordinates which is attached to each cross-section. Before deformation, the $\hat{x}_B$, $\hat{y}_B$, $\hat{z}_B$ directions are parallel to the x,y,z directions, respectively. Since the in-plane warping is neglected, the entire cross-section is deformed "rigidly" (note that the out-of-plane warping does not vanish) to its new position. The deformed orientation of the triad $\hat{x}_B$, $\hat{y}_B$, $\hat{z}_B$ is a function of the displacements u, v, w and ϕ and their derivatives, and is denoted $\hat{x}_D$, $\hat{y}_D$, $\hat{z}_D$. The above cross-sectional systems before and after deformation are related by a nonlinear transformation matrix (see Ref. 16). The following derivation is based on Green strain tensor components (see Ref. 17), namely:

$$\varepsilon_{ij} = \frac{1}{2}\left(\vec{G}_i \cdot \vec{G}_j - \vec{g}_i \cdot \vec{g}_j\right) \qquad (i,j = x,y,z) \qquad (1)$$

where $\vec{G}_i$, $\vec{G}_j$ and $\vec{g}_i$, $\vec{g}_j$ are the tangent base vectors before and after deformation. The constitutive relations for a general orthotropic laminae having a principal axis which does not coincide with the x direction are assumed to be of the form:

$$\{\sigma\} = [C']\{\varepsilon\} \qquad (2)$$

where $\{\sigma\}$ and $\{\varepsilon\}$ are the stress and strain vectors, respectively:

$$\{\sigma\} = \langle \sigma_{xx}, \sigma_{yy}, \sigma_{zz}, \tau_{yz}, \tau_{xz}, \tau_{xy} \rangle \qquad (3a)$$

$$\{\varepsilon\} = \langle \varepsilon_{xx}, \varepsilon_{yy}, \varepsilon_{zz}, \gamma_{yz}, \gamma_{xz}, \gamma_{xy} \rangle \qquad (3b)$$

In the following derivation only the stress components σ_{xx}, τ_{xz}, τ_{xy} will be of interest. Based on the above constitutive relations, these stress components may be expressed as:

$$\begin{Bmatrix} \sigma_{xx} \\ \tau_{xz} \\ \tau_{xy} \end{Bmatrix} = [C_1] \begin{Bmatrix} \varepsilon_{xx} \\ \gamma_{xz} \\ \gamma_{xy} \end{Bmatrix} + \underline{[C_2] \begin{Bmatrix} \varepsilon_{yy} \\ \varepsilon_{zz} \\ \gamma_{yz} \end{Bmatrix}} \qquad (4)$$

Essentially, the strain components ε_{yy}, ε_{zz}, γ_{yz} contain only small nonlinear contributions due to the neglect of the inplane deformation. Therefore, by ignoring the underlined part in Eq. (4), it becomes

the reduced constitutive relations for this case. However, these relations do not account for Poisson's effect. To correct this deficiency, the strain components ε_{yy}, ε_{zz}, γ_{yz} may be written as function of the stress components σ_{xx}, τ_{xz}, τ_{yz} by neglecting the normal stresses σ_{yy}, σ_{zz} and the shear stress τ_{yz} (see also Refs. 12,15), which yields the following new stress-strain relations:

$$\begin{Bmatrix} \sigma_{xx} \\ \tau_{xz} \\ \tau_{xy} \end{Bmatrix} = [C] \begin{Bmatrix} \varepsilon_{xx} \\ \gamma_{xz} \\ \gamma_{xy} \end{Bmatrix} \tag{5}$$

where

$$[C] = \{[I] - [C_2][S]\}^{-1} [C_1] = \begin{bmatrix} C_{11} & 0 & C_{16} \\ 0 & C_{55} & 0 \\ C_{16} & 0 & C_{66} \end{bmatrix} \tag{6}$$

where the matrix [S] contains elements of the compliance matrix associated with [C'].

Linear reduction of the strains which are determined by Eq. (1) shows that the only nonzero linear strains are:

$$\varepsilon^{L}_{xx} = u_{,x} - yv_{,xx} - zw_{,xx} + \psi_{,x} \tag{7a}$$

$$\gamma^{L}_{xz} = y\phi_{,x} + \psi_{,z} \tag{7b}$$

$$\gamma^{L}_{xy} = -z\phi_{,x} + \psi_{,y} \tag{7c}$$

As will be explained in what follows, the nonlinear strains contributions ε^{N}_{xx}, γ^{N}_{xz}, γ^{N}_{xy} are obtained implicitly by subtracting the above linear strains from the complete strains expressions. Thus, by substituting ε^{L}_{xx}, γ^{L}_{xz}, γ^{L}_{xy} in the constitutive relations (Eq. (5)), the linear stresses components σ^{L}_{xx}, τ^{L}_{xz}, τ^{L}_{xy} are obtained, and similarly, by substituting ε^{N}_{xx}, γ^{N}_{xz}, γ^{N}_{xy} in these relations, the nonlinear stresses components σ^{N}_{xx}, τ^{N}_{xz}, τ^{N}_{xy} are obtained.

At this stage, it is possible to express the axial resultant force, the transverse resultant forces and the resultant torsional moment that act at each cross-section in the deformed directions, in terms of the above stresses. Within the small strains assumption, the stress vector at each point is given by (see Ref. 17):

$$\vec{t} = \sqrt{\vec{g}_x \cdot \vec{g}_x}\,(\sigma_{xx}\vec{G}_x + \tau_{xy}\vec{G}_y + \tau_{xz}\vec{G}_z) \tag{8}$$

By expressing the base vectors $\vec{G}_i$ as sums of unit vectors in the deformed directions and nonlinear contributions $\vec{G}^{N}_i$, the nonlinear stresses t^{N}_x, t^{N}_y and t^{N}_z are obtained. Consequently, the linear and nonlinear loads that act at each cross-section may be expressed by the following integrations over each cross-sectional area:

$$(F^{L}_x, F^{N}_x) = \iint_A (\sigma^{L}_{xx}, t^{N}_x)dA \tag{9a}$$

$$(F^{L}_y, F^{N}_y) = \iint_A (\tau^{L}_{xy}, t^{N}_y)dA \tag{9b}$$

$$(F^{L}_z, F^{N}_z) = \iint_A (\tau^{L}_{xz}, t^{N}_z)dA \tag{9c}$$

$$(M^{L}_x, M^{N}_x) = \iint_A (\tau^{L}_{xz}\, y - \tau^{L}_{xy}\, z,\ t^{N}_z\, y - t^{N}_y\, z)dA \tag{9d}$$

As already mentioned, the out-of-plane warping function ψ is a three-dimensional function and has a local nature (i.e. it is also a function of the cross-sectional coordinates y_D and z_D). Consequently, a local equation is required for a consistent determination of this function. This local equation turns out to be the differential equilibrium equation in the axial direction (while the other two differential equations are fulfilled in an integral manner by Eqs. (9b-c)). This equation may be generally expressed as:

$$\sigma_{xx,x_D} + \tau_{xy,y_D} + \tau_{xz,z_D} + B_x = 0 \tag{10}$$

where B_x is the axial body force (in $\hat{x}_D$ direction). In the case of rotating blades, this body force may play an important role and should be accounted for. Using Eqs. (5),(6),(7) enables to rewrite Eq. (10) as:

$$\frac{dx}{dx_D}\left[C_{11}(u_{,xx}-yv_{,xxx}-zw_{,xxx}+\psi_{,xx})+C_{16}(-z\phi_{,x}+\psi_{,xy})\right]+$$

$$+ C_{16}(-v_{,xx}+\psi_{,xy})+C_{16,y}(u_{,x}-yv_{,xx}-zw_{,xx}+\psi_{,x})+C_{66}\psi_{,yy}$$

$$+ C_{66,y}(-z\phi_{,x}+\psi_{,y})+C_{55}\psi_{,zz}+C_{55,z}(y\phi_{,x}+\psi_{,z})= -B_x-B_x^N \qquad (11)$$

where B_x^N (which contains the nonlinear stress contributions) and $\frac{dx}{dx_D}$ are given in Ref. 15.

The Finite-Differences Formulation

As shown schematically by Fig. 2a, each cross-section of the beam is divided into a net of rectangular cells. This net must not be uniform over the cross-section but it is identical for each cross-section along the beam. Figure 2a presents a generic cross-section which is divided into equal square cells. At the middle point of each cell, a value is assigned to the out-of-plane warping function, ψ. The cells are numbered so the value ψ_n stands for the warping at the middle of the n^{th} cell. The total number of cells in the cross-section is denoted by N. Consequently, Eqs. (9a-d) and (11) may be put in a form of a linear system of equations:

$$[R]\{u\} = \{f\} \qquad (12)$$

where the unknowns vector and the right-hand side vector are given by:

$$\{u\} = \langle u_{,x},\ v_{,xxx},\ w_{,xxx},\ \phi_{,x},\ \psi_1,\ \psi_2 \ldots \psi_N \rangle \qquad (13a)$$

$$\{f\} = \langle z_1,\ z_2,\ z_3,\ z_4,\ f(1) \ldots\ldots f(N) \rangle \qquad (13b)$$

All nonlinear terms and linear terms which are not functions of the unknowns vector {u} are moved to the {f} vector. It should be noted that the specific choice of the above unknowns vector involves various considerations. The most important considerations were the ability to have a nonsingular matrix in the most simple cases of isotropic symmetric cross-sections, and the need to include explicitly as unknowns high derivatives of the displacements (i.e. $v_{,xxx}$, $w_{,xxx}$) in order to minimize the required numerical differentiations.

The elements of [R] that contain derivatives of ψ with respect to y_D or z_D are determined by a finite-difference scheme. In order to write the warping derivatives over the cross-sectional contour, the cross-sectional boundary conditions should be dealt with. These cross-sectional boundary conditions are Neumann-type conditions for the first derivative of the warping and are set by requiring no shear stress in a direction which is normal to the cross-sectional contour (see Fig. 2b). For example, for a vertical contour line, Eq. (5) shows that for $\tau_{xy} = 0$:

$$(\psi_{,y})_B = E_y - \frac{C_{16}}{C_{66}} u_{,x} + z\phi_{,x} \qquad (14)$$

where E_y is also a function of the displacements and their derivatives. Since expressing the first and the second derivatives by central finite differences is based on the point where the derivative is calculated, and two additional points one on each side of it, the boundary points need special care. Referring to Fig. 2c, it may be shown that knowing the value of the first derivative with respect to y at the boundary points B, enables to express the first and second derivative with respect to y at point 1 as:

$$(\psi_{,y})_1 = a_1(\psi_{,y})_B + b_1\psi_1 + c_1\psi_2 \qquad (15a)$$

$$(\psi_{,yy})_1 = a_2(\psi_{,y})_B + b_2\psi_1 + c_2\psi_2 \qquad (15b)$$

where $a_1, a_2, b_1, b_2, c_1, c_2$ depend on the cells dimensions. Similar procedures apply to the derivatives in the z direction.

Solution Procedure

Generally, the overall three-dimensional solution is achieved by an iterative procedure which basically consists of successive solutions of Eq. (12) at each cross-section. In order to describe this process, the following discussion will be concentrated on the case of a cantilevered beam which will also clarify the application of the present method to other boundary conditions.

The beam is assumed to undergo a distribution of body force B_x in the $\hat{x}_D$ direction, transverse forces per unit length p_y and p_z in the $\hat{y}_D$ and $\hat{z}_D$ directions, respectively, and a distribution of moments per unit length q_x, q_y and q_z in the $\hat{x}_D$, $\hat{y}_D$, $\hat{z}_D$ directions, respectively. All loads are assumed to be given as functions of x. In addition, the tip resultant forces and moments $\vec{F}^t$, $\vec{M}^t$ are prescribed over the tip cross-section.

The solution procedure consists of the following four steps:

Step 1 - Determination of the loads distribution: Based on some initially assumed distribution of displacements, the above tip and distributed loads are determined. These loads are then integrated to give the resultant loads at each cross-section in the $\hat{x}_D$, $\hat{y}_D$, $\hat{z}_D$ directions.

Step 2 - Determination of the nonlinear contributions: For this purpose, the base vectors $\vec{G}_i$, $\vec{g}_i$ are determined including the nonlinear contributions $\vec{G}^N_i$. Then, the strains ε_{ij} are calculated (Eq. (1)) and the nonlinear components ε^N_{xx}, ε^N_{xz}, ε^N_{xy} are obtained by subtracting the linear stresses ε^L_{xx}, ε^L_{xz}, ε^L_{xy} (Eqs. (7a-c). Consequently, the nonlinear stresses σ^N_{xx}, τ^N_{xz}, τ^N_{xy} may be determined (using Eq. (5)), and the nonlinear components t^N_x, t^N_y, t^N_z of the stress vector are evaluated. Finally the nonlinear resultant loads F^N_x, F^N_y, F^N_z, M^N_x (Eqs. 9a-d) and the nonlinear body force B^N_x are determined.

Step 3 - Determination of the unknowns vector: Using the above linear and nonlinear loads, and based on the above initially assumed displacements, the right-hand side of Eq. (12) is determined for each cross-section. Then, Eq. (12) is solved for each cross-section and the local values of the unknown vector {u} are obtained.

Step 4 - Updating the displacements assumption: The components of {u} are differentiated and/or integrated along the beam span and the values of u, $u_{,xx}$, v, $v_{,x}$, $v_{,xx}$, w, $w_{,x}$, $w_{,xx}$, ϕ, $\phi_{,xx}$, $\psi_{,x}$ and $\psi_{,xx}$ are obtained. Differentiations are executed by central finite-differences scheme. Integration constants are obtained by the global boundary conditions of the beam. Note that one aspect of the boundary conditions has been already discussed and introduced to the scheme by demanding that there will be no shear stresses over the outer surface area of the beam. In addition to these local boundary conditions, and according to the above beam-like behavior assumption, the global displacements unknowns u, v, w and ϕ are subjected to the global boundary conditions. At the root (x=0), the geometrical boundary conditions for a clamped beam are:

$$u = v_{,x} = v = w_{,x} = w = \phi = 0 \qquad (16)$$

The natural boundary conditions for $v_{,xx}$ and $w_{,xx}$ are given at the tip and are obtained by equating the tip transverse moments obtained by integrations of the normal stresses to the external moments M^t_y, M^t_z, respectively. This yields the following system of two equations and unknowns:

$$\begin{bmatrix} T_{11} & T_{12} \\ T_{21} & T_{22} \end{bmatrix} \begin{Bmatrix} v_{,xx(L)} \\ w_{,xx(L)} \end{Bmatrix} = \begin{Bmatrix} R_y \\ R_z \end{Bmatrix} \qquad (17)$$

where T_{11},T_{12},T_{21},T_{22},R_y and R_z are given in Ref. 15.

Step 4 provides updated values to the initially assumed displacements, and the above procedure is repeated until convergence is achieved.

Results

This section documents some analytic solutions for generic cross-sections and typical numerical results which were obtained for a clamped-free composite beam of a rectangular cross-section. In all cases the beams are made of Graphite/Epoxy orthotropic laminae. All geometric and material properties are given in Appendix A. In the numerical examples, a net of 10x20 cells has been used to discretize the cross-sectional area while 20 equally spaced cross-sections were considered along the beam axis. The cross-sectional discretization is presented in Figs. 3a,b for a homogeneous beam and for a beam with two lamina. As shown, the cross-section dimensions are a and b (parallel to y_D and z_D directions, respectively), and is discretized by a "cosine rule" which creates smaller cells along the boundaries of each lamina.

Homogeneous Beams (analytic solutions):

Homogeneous beams may be viewed as beams made of identical laminae oriented at the same angle or as beams made of a single lamina. The present formulation yields some exact linear analytic solutions for this case. The linear version of the above formulation shows that the functions u(x), v(x), w(x), ϕ(x) and ψ(x,y,z) form an exact solution provided that they satisfy the linear part of Eqs. (9a-d) and (10), satisfy the cross-sectional boundary conditions (such as Eq. (14)), the global boundary conditions (Eqs. (16) and (17)), and ψ has zero averaged value over the cross-section. In all cases, it has been assumed that the $\hat{x}_D$, $\hat{y}_D$ and $\hat{z}_D$ system of coordinates is located at the cross-sectional centroid. A detailed derivation may be found in Ref. 15.

Case a - Tensile Force (generic cross-section): In this example, it is assumed that the beam is subjected to a tensile force, P(x), which is created by a tip force and a distribution of body force in the x direction. The solution in this case is given by $w=\phi=0$ and (see also Fig. 4):

$$\psi = - \frac{P(x)}{A} \frac{C_{16}}{C_{11}C_{66}-C_{16}^2} y \qquad (18a)$$

$$v_{,xx} = - \frac{P(x)_{,x}}{A} \frac{C_{16}}{C_{11}C_{66}-C_{16}^2} \qquad (18b)$$

$$u_{,x} = \frac{P(x)}{A} \frac{C_{66}}{C_{11}C_{66}-C_{16}^2} \qquad (18c)$$

The expressions for u, $v_{,x}$ and v are easily obtained by introducing the appropriate boundary conditions for u(o), v(o), $v_{,x}$(o).

Case b: Tip Torsional Moment (generic cross-section): Exact analytic linear solution for a cantilever beam which is subjected to a tip twist moment, M, is presented in this section. The solution in this case is based on the solution of a special orthotropic beam where the plane normal to the beam axis is a plane of elastic symmetry (see Ref. 18). This case may be obtained by the present formulation by setting $C_{16}=0$ which decouples twist and bending. Thus, it is assumed that the warping function $\varphi(y,z)$ (defined by $\psi(y,z)=\phi_{,x}\varphi(y,z)$ and the rigidity D (defined by $M=\phi_{,x}D$) of such an uncoupled case are known for the actual values of C_{55} and C_{66}. The twist and the warping in the coupled case take the form:

$$\phi_{,x} = \frac{M}{D} + \alpha \qquad (19a)$$

$$\psi = \frac{M}{D} \varphi_{(y,z)} - \alpha yz + A_\psi y^2 + B_\psi y + C_\psi \qquad (19b)$$

and for a clamped beam where the z axis is a symmetry axis, the solution is given by:

$$w = - \frac{M}{D} \frac{C_{16}C_{66}}{2(C_{11}C_{66}-C_{16}^2)} r_z x^2 \qquad (20a)$$

$$\phi = \frac{M}{D} \left[1 + \frac{C_{16}^2}{2(C_{11}C_{66}-C_{16}^2)} r_z\right] x \qquad (20b)$$

which enables clear insight into this Torsion-Bending coupling mechanisms. The expressions for A_ψ, B_ψ and C_ψ are given in Ref. 15.

For a rectangular cross-section r_z, is given by (see Fig. 5):

$$r_z = 2 - \frac{192}{q\pi^2} \sum_{n=0}^{\infty} \frac{(-1)^n}{(2n+1)^4} \tanh(mq)\left[\frac{1}{m} \sin(m)-\cos(m)\right] \qquad (21a)$$

where

$$m = \frac{2n+1}{2} \pi \qquad (21b)$$

q is a nondimensional parameter which accounts for the cross-sectional thickness ratio and its anisotropy, and is given by:

$$q = \frac{a}{b} \sqrt{\frac{C_{55}}{C_{66}}} \qquad (22)$$

For an elliptical cross-section of axes a and b (parallel to y and z direction, respectively), r_z is given by:

$$r_z = \frac{2q^2}{1+q^2} \qquad (23)$$

The warping distribution for the case of a rectangular cross-section is presented in Fig. 6.

Case c - Vertical Load (rectangular cross-section): An analytic solution for a beam having a rectangular cross-section and subjected to a vertical load $F_z(x)$ (in the z direction) is described in this section. The solution in this case shows that u=v=0, and:

$$\psi = - \frac{6F_z}{ab^3C_{55}} \left[\frac{z^3}{3} - \left(\frac{b}{2}\right)^2 z\right] - \phi_{,x} yz \qquad (24a)$$

$$w = \frac{2F_z}{ab^3} \frac{C_{66}}{C_{11}C_{66}-C_{16}^2} x^2(3L-x) \qquad (24b)$$

$$\phi = -\frac{3F_z}{ab^3}\frac{C_{16}}{C_{11}C_{66}-C_{16}^2}x(2L-x) \qquad (24c)$$

Again, the Torsion-Bending coupling is clearly presented by the above result.

Case d - Tip Edgewise Load (rectangular cross-section): If a beam of rectangular cross-section is subjected to a tip edgewise load, F_y (in the y direction), an exact linear analytic solution may be obtained by assuming $w=\phi=0$, and warping distribution of the following form:

$$\psi=A_\psi\left[\frac{y^3}{3}-\left(\frac{a}{2}\right)^2 y\right]+B_\psi y^3+C_\psi(x-L)(y^2-\frac{a^2}{12})+D_\psi y \qquad (25)$$

where the expressions for the above coefficients may be found in Ref. 15. For a clamped beam, u and v are given by:

$$v = \frac{2F_y}{a^3 b}\frac{C_{66}}{C_{11}C_{66}-C_{16}^2}x^2(3L-x) \qquad (26a)$$

$$u = -\frac{F_y}{ab}\frac{1}{C_{11}\frac{C_{66}}{C_{16}}-C_{16}}x \qquad (26b)$$

Non-Homogeneous Beam (numerical solutions):

In the following discussion, a beam made of two laminae of equal thickness is dealt with. The cross-sectional discretization is presented in Fig. (3b). The principal orthotropic axes of the lower and upper laminae are assumed to create angles θ and $-\theta$, respectively, with the beam axis, while for $\theta=0$ both laminae are identical. This case is usually referred to as "antisymmetric".

First, a demonstration of the Extension-Torsion mechanism in this beam will be presented. The results of applying tension force at the tip, P, appear in Fig. 7 where the tip extension u_t (normalized by its value for $\theta=0$) and the tip twist angle per unit tensile force are presented as function of θ. As expected, u_t is growing with θ due to the reduction in the longitudinal stiffness of the beam. The twist angle, $\phi_{,x}$, is growing up to its maximum value (about -7.5×10^{-4} deg./Nt) around $\theta=40$ degrees.

The warping distribution in this case is presented in Fig. 8. As shown, there is an opposite trend in the out-of-plane warping of the two laminae. As a result, interlaminar stresses are created. These stresses are the τ_{xz} components over the laminae contact surface (z=0) which are presented in Fig. 9. As shown, these interlaminar stresses are larger close to the cross-sectional vertical boundaries and reach a maximum value of about 40% of the averaged axial stress.

Concluding Remarks

A formulation and a solution procedure which are capable of determining the structural behavior of orthotropic beams having solid cross-section have been presented. It has been shown that it is possible to obtain a solution which includes a detailed description of the out-of-plane warping and all three dimensional effects. Due to the detailed description of the warping, prediction of the interlaminar stresses in multilayered beams are provided as well. In addition, the introduction of the axial body forces which is carried out by the differential equilibrium equation, contributes to the quality of the results obtained for rotating blades.

The present formulation also provides some closed-form "strength of material type" analytic solutions for homogeneous beams which lay down an important insight into the composite-related coupling effects.

References

1. Hong, C.H. and Chopra, I., "Aeroelastic Stability of a Composite Blade", *Journal of the American Helicopter Society*, Vol. 30, No. 2, April 1985.

2. Panada, B. and Chopra, I., "Dynamics of Composite Rotor Blades in Forward Flight", *Vertica*, Vol. 11, Nos. 1/2, 1987.

3. Hodges, D.H., "Review of Composite Rotor Blade Modelling", *AIAA Journal*, Vol. 28, No. 3, pp. 561-565, March 1990.

4. Crespo da Silva, M.R.M., "Equations for Nonlinear Analysis of 3D Motions of Beams", *Appl. Mech. Rev.*, Vol. 44, No. 11, Part 2, Nov. 1991.

5. Kapania, R.K. and Raciti, S., "Recent Advances in Analysis of Laminated Beams and Plates, Part I: Shear Effects and Buckling", *AIAA Journal*, Vol. 27, No. 7, pp. 923-934, July 1989.

6. Giavotto, V., Borri, M., Mantegazza, P., Ghiringhelli, G., Carmaschi, V., Maffioli, G.C. and Mussi, F., "Anisotropic Beam Theory and Applications", *Computers and Structures*, Vol. 16, 1983, pp. 402-413.

7. Borri, M. and Mantegazza, P., "Some Contributions on Structural and Dynamic Modeling of Rotor Blades", *l'Aerotecnica Missili e Spazio*, Vol. 64, No. 9, 1985, pp. 143-154.

8. Lee, S.W. and Kim, Y.H., "A New Approach to the Finite-Element Modeling of Beams with Warping Effects", *Int. J. Num. Math. Eng.*, Vol. 24, pp. 2327-2341, 1987.

9. Stemple, A.D. and Lee, S.W., "Large Deflection Static and Dynamic Finite Element Analysis of Composite Beams with Arbitrary Cross-Sectional Warping", *AIAA Paper No. 89-1363-CP*, Pro. 30th AIAA/ASME/ASCE/AHS/ACS Structures, Structural Dynamics and Materials Conf., Mobile, AL, April 1989, pp. 1788-1798.

10. Bauchau, O.A., "A Beam Theory for Anisotropic Materials", *J. of Appl. Mechanics*, Vol. 52, 1985, pp. 416-422.

11. Bauchau, O.A. and Hong, C.H., "Finite Element Approach to Rotor Blade Modeling", *J. of the American Helicopter Society*, Vol. 32, No. 1, 1987, pp. 60-67.

12. Kosmatka, J.B. and Friedmann, P.P., "Structural Dynamic Modeling of Advanced Composite Propellers by the Finite Element Method", *Proceedings of the 28th AIAA/ASME/ASCE/AHS Structures, Structural Dynamics and Materials Conference*, Monterey, California, April 1987.

13. Kosmatka, J.B. and Friedmann, F.P., "Vibration Analysis of Composite Turbopropellers Using a Nonlinear Beam-Type Finite Element Approach", *AIAA Journal*, Vol. 27, No. 11, Nov. 1989.

14. Atilgan, A.R., Hodges, D.G. and Fulton, M.Y., "Nonlinear Deformation of Composite Beams: Unification of Cross-Sectional and Elastic Analysis", *Appl. Mech. Rev.*, Vol. 44, No. 11, Part 2, Nov. 1991.

15. Rand, O., "Nonlinear Analyses of Orthotropic Beams of Solid Cross-Sections", To appear in the *Journal of Composite Structures.*

16. Rosen, A. and Rand, O., "A General Model of the Dynamics of Moving and Rotating Rods", *Computers and Structures*, Vol. 21, No. 3, pp. 543-561, 1985.

17. Wempner, G., "*Mechanics of Solids with Applications to Thin Bodies*", McGraw-Hill Book Co., 1973.

18. Sokolnikoff, I.S., "*Mathematical Theory of Elasticity*", 2nd Ed. McGraw-Hill Book Co., 1956.

Appendix A. Geometric and Material Properties

The numerical examples presented in this paper are for a cantilevered beam of length L, and cross-sectional dimensions a and b where:

$$L = 0.4 \text{ m} \tag{A.1}$$

$$a = 0.02 \text{ m} \tag{A.2}$$

$$b = 0.01 \text{ m} \tag{A.3}$$

a,b and the location of the cross-sectional system of coordinates are presented in Fig. 3. The beam was made of Graphite/Epoxy laminae of the following characteristics:

$$E_{11} = 129.1 \times 10^9 \text{ N/m}^2 \tag{A.4}$$

$$E_{22} = E_{33} = 9.4 \times 10^9 \text{ N/m}^2 \tag{A.5}$$

$$G_{12} = 5.5 \times 10^9 \text{ N/m}^2 \tag{A.6}$$

$$G_{13} = 4.3 \times 10^9 \text{ N/m}^2 \tag{A.7}$$

$$G_{23} = 2.5 \times 10^9 \text{ N/m}^2 \tag{A.8}$$

$$\nu_{12} = \nu_{13} = 0.3 \tag{A.9}$$

$$\nu_{23} = 0.5 \tag{A.10}$$

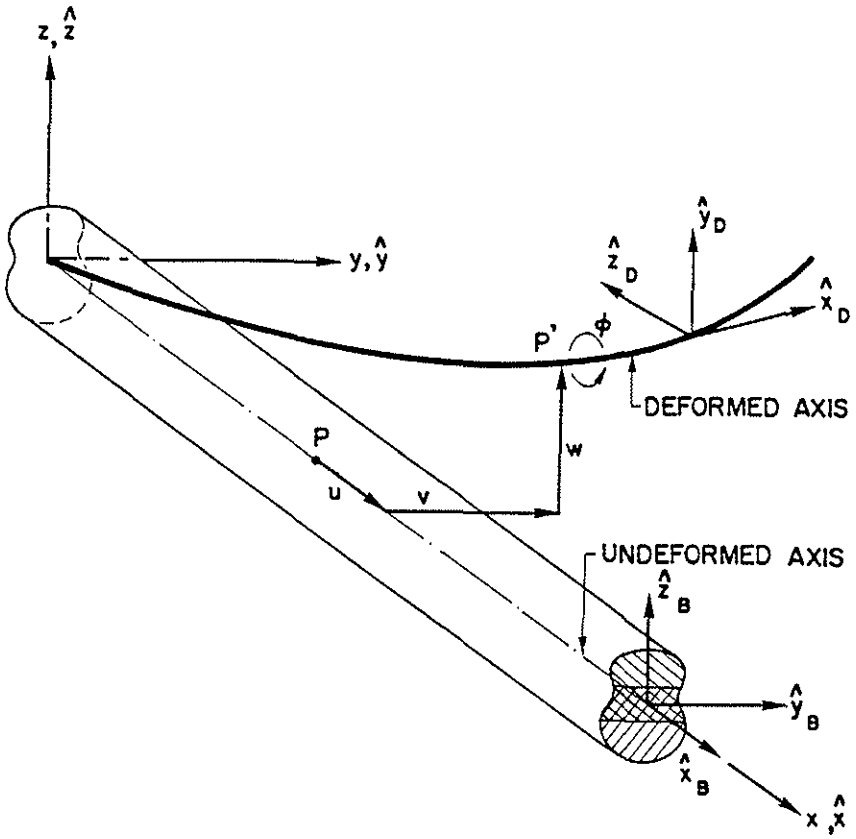

Fig. 1: Scheme of the undeformed beam, the deformed axis and the systems of coordinates.

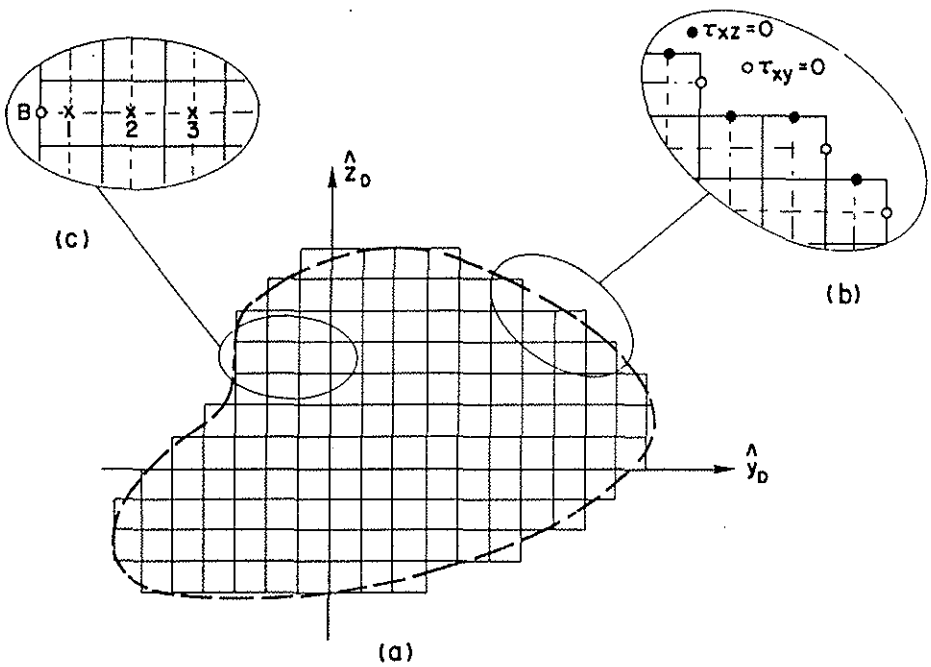

Fig. 2: Scheme of the cross-sectional discretization.

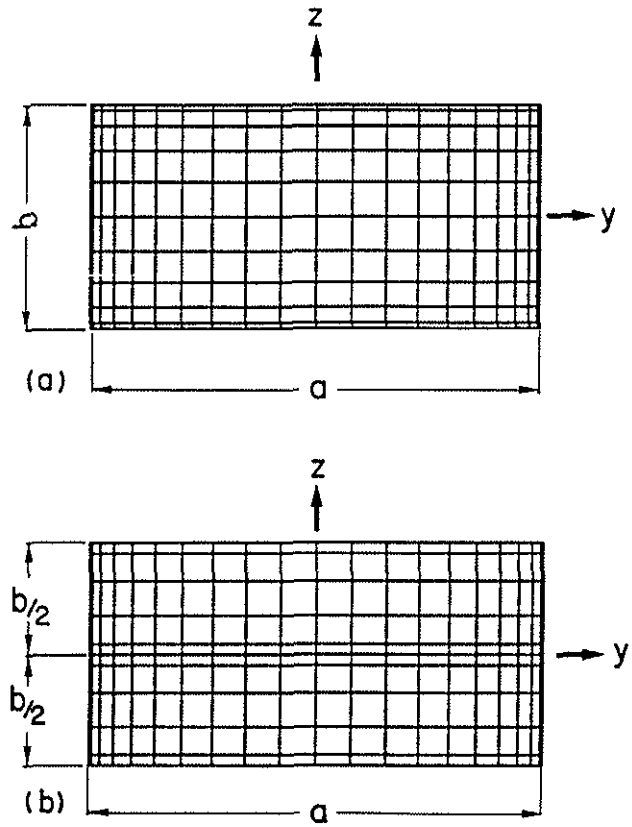

Fig. 3: Discretization of a rectangular cross -section:
(a) Homogeneous beam
(b) A beam of two laminae.

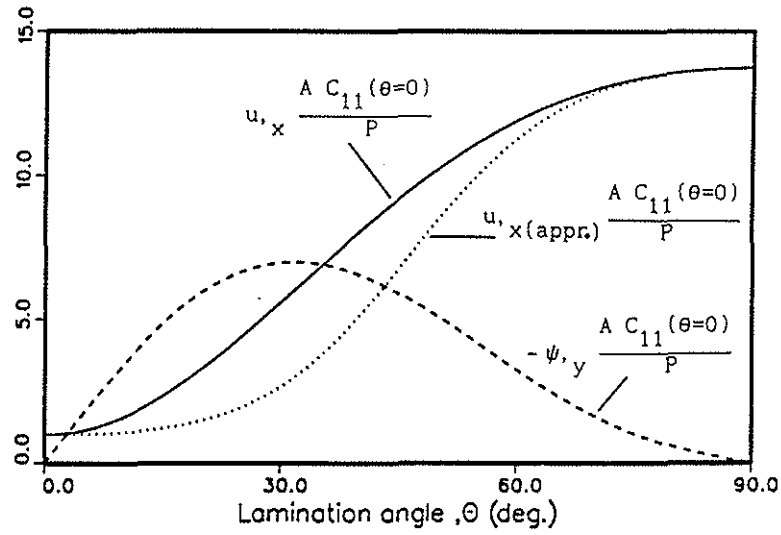

Fig. 4: The values of $u_{,x}$ and $\psi_{,y}$ due to a tip tensile force as function of the lamination angle in homogeneous beam and the approximate value based on $u_{,x}=P/(AC_{11})$.

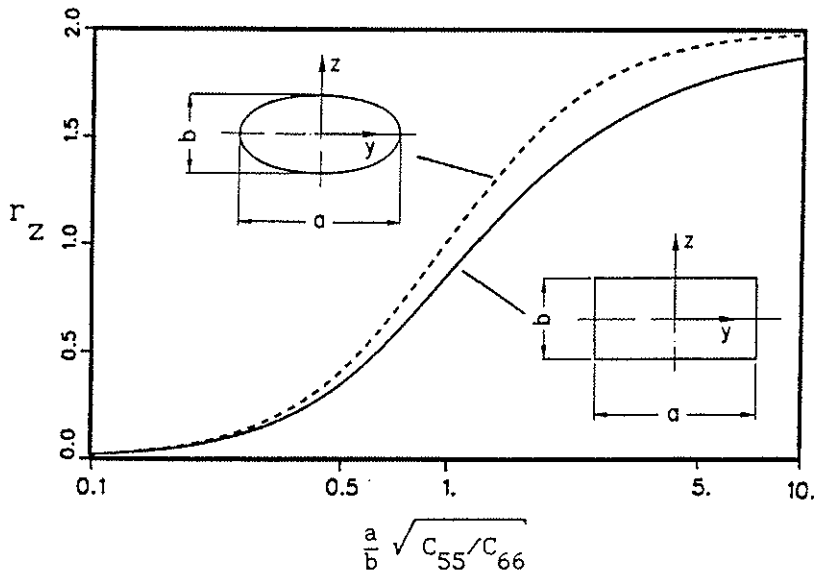

Fig. 5: Variations of r_z as a function of $\frac{a}{b}\sqrt{C_{55}/C_{66}}$ for homogeneous rectangular and elliptic cross-sections.

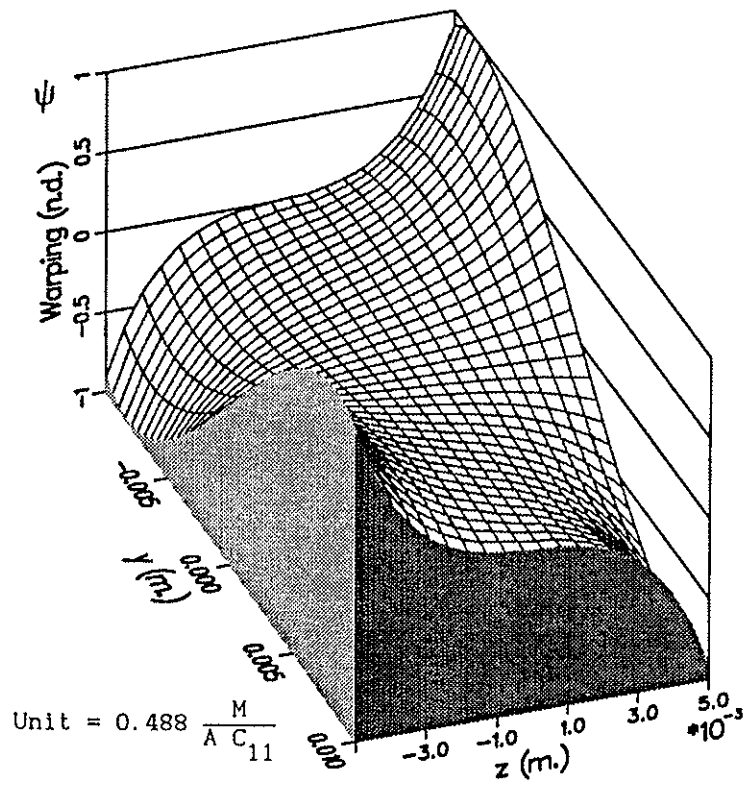

Fig. 6: Warping distribution due to a tip torsional moment in homogeneous beam (θ=30 , x=L/2).

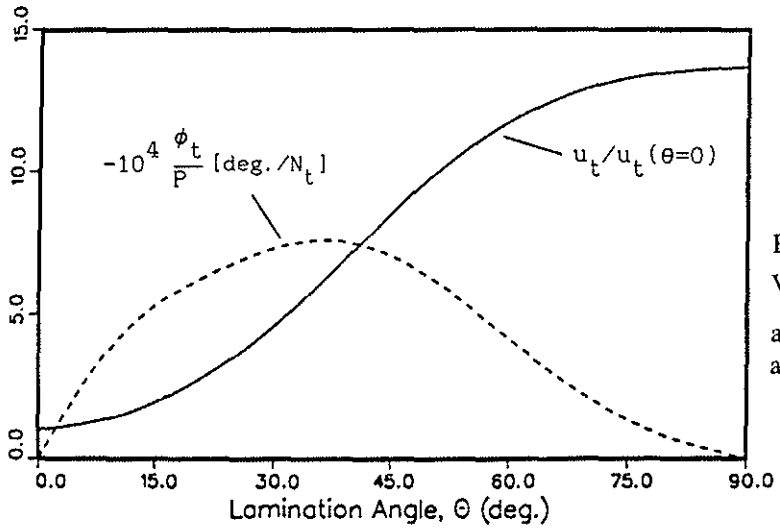

Fig. 7:
Variation of the tip values u_t and ϕ_t due to a tip tensile force in an antisymmetric beam as function of the lamination angle.

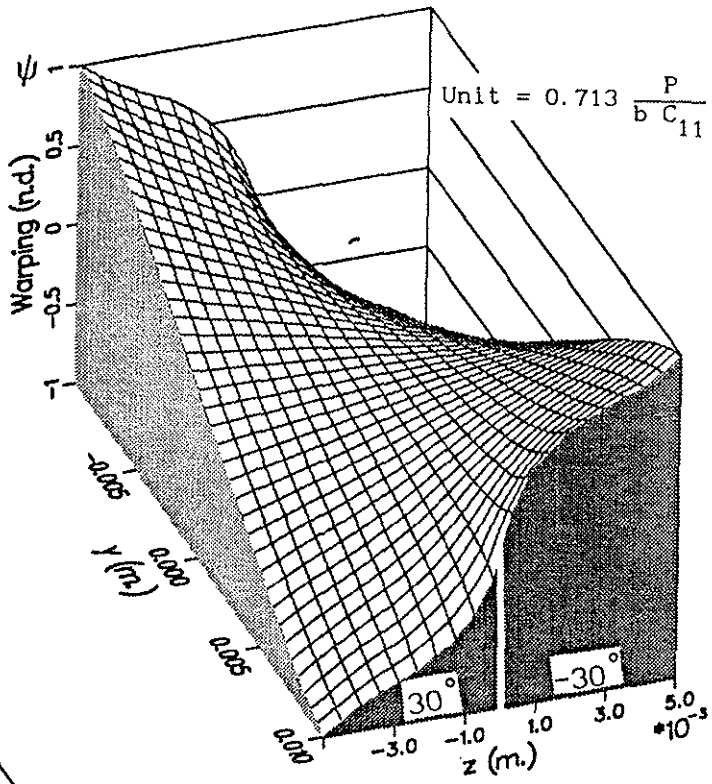

Fig. 8:
Warping distribution due to a tip tensile force in an antisymmetric beam.

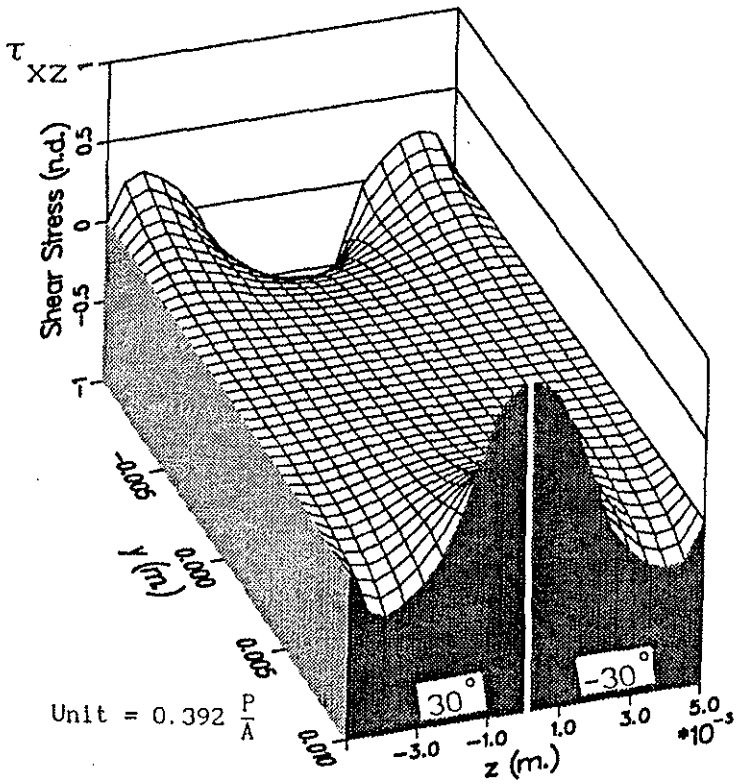

Fig. 9:
Distribution of the τ_{xz} shear stress due to a tip tensile force in an antisymmetric beam.